

DMD #55400

Amlodipine metabolism in human liver microsomes and roles of CYP3A4/5 in the dihydropyridine dehydrogenation

Yanlin Zhu, Fen Wang, Quan Li, Mingshe Zhu, Alicia Du, Wei Tang, Weiqing Chen

DMPK Dept, Shanghai ChemPartner, Shanghai (Y.Z., F.W., Q.L., A.D., W.T., W.C.): Dept of Biotransformation Dept, Bristol-Myers Squibb, Princeton (M.Z.)

DMD #55400

Running Title: Metabolism of amlodipine by HLM and CYP3A4

Address correspondence to:

Weiping Chen, DMPK Dept, Shanghai ChemPartner, 998 Halei Rd, Zhangjiang Hi-tech PK, Pudong New Area, Shanghai 201203, PR China. Email: weiqingchen@chempartner.cn

Mingshe Zhu, Biotransformation Dept, Bristol-Myers Squibb, Princeton, NJ 08543. E-mail:mingshe.zhu@bms.com.

The number of text pages: 17

The number of tables: 1

The number of figures: 3

The number of references: 18

The number of words in the Abstract: 242

The number of words in the Introduction: 615

The number of words in Discussion: 947

Abbreviations:

Area under the curve (AUC)

Drug-drug interaction (DDI)

Human liver microsomes (HLM)

Liquid chromatography (LC)

Mass spectrometry (MS)

1'-Hydroxy-midazolam (1'-OH-midazolam)

N,N',N'-triethylenethiophosphoramidate (Thio-TEPA)

Reduced form of β -nicotinamide adenine dinucleotide phosphat (NADPH)

DMD #55400

ABSTRACT

Amlodipine is a commonly prescribed calcium channel blocker for the treatment of hypertension and ischemic heart disease. The drug is slowly cleared in human primarily via dehydrogenation of its dihydropyridine moiety to a pyridine derivative (M9). Results from clinical drug-drug interaction studies suggest that CYP3A4/5 mediate metabolism of amlodipine. However, attempts to identify a role of CYP3A5 in amlodipine metabolism in human based on its pharmacokinetic differences between CYP3A5 expressers and non-expressers failed. Objectives of this study were to determine metabolite profile of amlodipine (a racemic mixture and *S*-isomer) in human liver microsomes (HLM), and to identify the CYP enzyme(s) involved in the M9 formation. Liquid chromatography/mass spectrometry analysis showed that amlodipine was mainly converted to M9 in HLM incubation. M9 underwent further *O*-demethylation, *O*-dealkylation and oxidative deamination to various pyridine derivatives. This observation is consistent with amlodipine metabolism in human. Incubations of amlodipine with HLM in the presence of selective CYP inhibitors showed that both ketoconazole (an inhibitor of CYP3A4/5) and CYP3cide (an inhibitor of CYP3A4) completely blocked the M9 formation, while chemical inhibitors of other CYP enzymes had little effect. Furthermore, metabolism of amlodipine in expressed human CYP enzymes showed that only CYP3A4 had significant activity in amlodipine dehydrogenation. Metabolite profiles and CYP reaction phenotyping data of a racemic mixture and *S*-isomer of amlodipine were very similar. The results from this study suggest that CYP3A4 rather than CYP3A5 plays a key role in metabolic clearance of amlodipine in human.

DMD #55400

Introduction

Amlodipine, a dihydropyridine calcium channel blocker, is one of the most commonly prescribed drugs for the treatment of hypertension and ischemic heart disease. In clinic, amlodipine shows a long elimination half-life (35 h) after a single 10-mg intravenous dose (Abernethy, 1991), likely due to its high volume of distribution and a low rate of plasma clearance. The drug also exhibits a good oral bioavailability in the range of 52-88% following a single 10-mg oral dose to human subjects (Faulkner et al., 1986). After an oral dose of radiolabeled amlodipine to human, the total radioactivity recovery is 59.3% in urine and 23.4% in feces (Beresford et al., 1988a; Stopher et al., 1988). Similarly, 62% and 22.7% of a radiolabeled intravenous dose are recovered in human urine and feces, respectively. *S*-amlodipine is the active component of racemic amlodipine. There are no significant differences in pharmacodynamic and pharmacokinetic parameters after a single dose of 5-mg *S*-amlodipine and 10-mg amlodipine racemate (Kim et al., 2010). The amlodipine pyridine metabolite (Fig. 1C, M9), raised from dehydrogenation of the dihydropyridine moiety, and its derivatives are major drug-related components in human urine. The mass balance and metabolite profiling data suggest that amlodipine dehydrogenation to M9 followed by multiple oxidative reactions of M9 is the major clearance pathway of amlodipine in human. Similar metabolic pathways are observed in the rat and dog (Beresford et al., 1988b). It has been reported that many dihydropyridine analogues undergo CYP3A4-mediated dehydrogenation to form the corresponding pyridine metabolites in vitro (Guengerich et al., 1991). However, the information of in vitro metabolism of amlodipine in human, including CYP reaction phenotyping data, is not available in the literature.

Telaprevir, a potent inhibitor of both CYP3A4 and 3A5, increases amlodipine mean area under the curve (AUC) by 2.79-fold and mean half-life from 41.3 h to 95.1 h when the two drugs

DMD #55400

are co-administered (Lee et al., 2011). Similarly, combined dosing of indinavir and ritonavir, both of which are CYP3A inhibitors, increases the median amlodipine AUC₀₋₂₄ by 90% (Glesby et al., 2005). These clinical drug-drug interaction (DDI) observations suggest that CYP3A4/5 enzymes play significant roles in metabolic clearance of amlodipine in human. CYP3A4 and CYP3A5 are two major enzymes of the CYP3A family and have similar catalytic specificities. However, unlike CYP3A4, CYP3A5 is a polymorphic enzyme. To determine if CYP3A5 contributes the metabolism of amlodipine, pharmacokinetics of amlodipine in CYP3A5 non-expressers (CYP3A5*3/*3 carriers) and CYP3A5 expressers (CYP3A5*1/*1 and CYP3A5*1/*3 carriers) have been recently determined and compared to each other. After a single dose of amlodipine, its exposure in CYP3A5 expressers is slightly higher than that in CYP3A5 non-expressers (Kim et al., 2006). However, the AUC and the maximal concentrations of amlodipine in CYP3A5 non-expressers are about two-fold higher than those in CYP3A5 expressers after 5-mg once-daily oral doses for seven days (Zuo et al., 2013). Although roles of CYP3A5 in the disposition and elimination of amlodipine in human have been suggested by investigators of these clinical studies, it is very challenging to draw meaningful conclusions without *in vitro* CYP phenotyping data of amlodipine. Furthermore, several studies have investigated the role of CYP3A5 polymorphism in blood pressure response to amlodipine, but results are not consistent (Zhang et al., 2013). The major objectives of this study were to determine amlodipine metabolite profile in human liver microsomes (HLM) and CYP enzyme(s) responsible for amlodipine dehydrogenation to M9. Especially, roles of CYP3A4 and CYP3A5 in amlodipine metabolism were investigated. In addition, *in vitro* metabolism of racemic amlodipine and S-amlodipine was compared to each other. Results from this study provide a biochemical basis for better

DMD #55400

understanding of the clinically observed amlodipine drug-drug interactions with CYP3A inhibitors and pharmacokinetics of amlodipine in both CYP3A5 non-expressers and expressers.

Materials and Methods

Chemicals and Reagents. A racemic amlodipine (2-[(2-Aminoethoxy)-methyl]-4-(2-chlorophenyl)-1,4-dihydro-6-methyl-3,5- pyridinedicarboxylic acid 3-ethyl 5-methyl ester benzene sulfonate Norvasc), quinidine, ketoconazole, N,N,N'-triethylenethiophosphoramidate (Thio-TEPA), montelukast, furafylline, sulfaphenazole, CYP3cide, and benzylnirvanol were purchased from Sigma (St. Louis, MO). *S*-amlodipine was purchased from Energy Chemical (Shanghai, China). All solvents (acetonitrile, methanol, and water) were of high-performance liquid chromatography (LC) grade. Pooled HLM was obtained from BD Biosciences (Woburn, MA). Expressed CYP enzymes, CYP-1A2, -2B6, -2C8, -2C9, -2C19, -2D6, -3A4, and -3A5 were purchased from BD Biosciences (San Jose, CA).

HLM Incubation for Metabolite Profiling. Racemic amlodipine and *S*-amlodipine (30 μ M) was separately incubated with HLM (2 mg protein/mL) for 60 min. The reaction mixtures (1 mL) also contained potassium phosphate buffer (69 mM, pH 7.4) and NADPH (4 mM). Metabolic reactions were initiated by addition of NADPH after 3 min pre-incubation and stopped by the addition of 2 mL of acetonitrile. Precipitate was removed by centrifugation. Supernatant was dried under nitrogen and then reconstituted in 200 μ l of 5% acetonitrile /water (v/v) for liquid chromatography/mass spectrometry (LC/MS) analysis.

Time Course of Amlodipine Metabolism in HLM. Racemic amlodipine and *S*-amlodipine (1 μ M) was separately incubated in duplicates in HLM (1 mg protein/mL) for 0, 5, 10, 15, 30, 60 min. The reaction mixtures (0.25 mL) also contained potassium phosphate buffer

DMD #55400

(69 mM, pH 7.4) and NADPH (2 mM). Metabolic reactions were initiated by addition of NADPH after 3 min pre-incubation and stopped at designated time points by addition of 0.5 mL of acetonitrile. Precipitate was removed by centrifugation. Supernatant was dried under nitrogen and then were reconstituted in 50 μ l of 5% acetonitrile /water (v/v) for determination of disappearance of the parent drug and the formation of the pyridine metabolite (M9).

Inhibition of Amlodipine Dehydrogenation HLM by CYP Inhibitors. Racemic amlodipine and *S*-amlodipine (1 μ M) was separately incubated in HLM (0.5 mg/mL) in triplicates for 13 min. Reaction mixtures (0.25 mL) also contained potassium phosphate buffer (69 mM, pH 7.4), a chemical inhibitor of CYP enzyme and NADPH (2 mM). Final concentrations of the CYP inhibitors were 1 μ M for benzylnirvanol, quinidine, ketoconazole, montelukast and CYP3c4, 10 μ M for furafylline and sulfaphenazole, and 50 μ M for Thio-TEPA. For the incubations with time-dependent inhibitors (Thio-TEPA, furafylline and CYP3c4), the reaction was initiated by addition of amlodipine or *S*-amlodipine after 10 min pre-incubations of HLM and NADPH in the presence of the individual CYP inhibitors. All of other reactions were initiated by addition of NADPH to after 3-min pre-incubations of HLM with amlodipine or *S*-amlodipine in the presence of the individual CYP inhibitors. All of the reactions were stopped by the addition of 0.5 mL of acetonitrile and the precipitate was removed by centrifugation. Supernatants were dried under nitrogen and then were reconstituted in 50 μ l of 5% acetonitrile /water (v/v) for LC/MS analysis.

Amlodipine Dehydrogenation by Expressed CYP Enzymes. Racemic amlodipine and *S*-amlodipine (1 μ M) were separately incubated with individual expressed human CYP enzymes (100 nM) (CYP1A2, -2B6, -2C8, -2C9, -2C19, -2D6, -3A4, and -3A5) in triplicates for 13 min. Reaction mixtures (0.25 mL) also contained potassium phosphate buffer (69 mM, pH 7.4) and

DMD #55400

NADPH (2 mM). After 3 min pre-incubation, metabolic reactions were initiated by addition of NADPH and stopped by the addition of 0.5 mL of acetonitrile. Precipitate was removed by centrifugation. The supernatant was dried under nitrogen and then was reconstituted in 50 μ L of 5% acetonitrile /water (v/v) for LC/MS analysis. In addition, racemic amlodipine was incubated with expressed CYP3A4 and CYP3A5 with or without CYP3cide under the conditions described above. In the same experiment, midazolam (10 μ M) was incubated with expressed CYP3A4 or CYP3A5 (100 nM) in triplicates for 5 min. Reaction mixtures (0.04 ml) also contained potassium phosphate buffer (69 mM, pH 7.4) and NADPH (2 mM). After 3 min pre-incubation, the metabolic reaction converting midazolam to 1'-hydroxy-midazolam (1'-OH-midazolam) was started by the addition of NADPH and stopped by the addition of 0.08 mL of acetonitrile. Precipitate was removed by centrifugation. Concentrations of 1'-OH-midazolam in the supernatant were quantitatively determined using LC/MS and 1'-OH-midazolam standard.

Liquid Chromatography/Mass Spectroemtry (LC/MS) Analysis. A LC/MS system consisted of an LC instrument (Thermo Accela HPLC with a photodiode array detector, Thermo Fisher Scientific, Waltham, MA) equipped with an Xbridge C18 column (5 μ m, 2.1 \times 150 mm, Waters, Milford, MA) and an ion trap mass spectrometer (LTQ XL, Thermo Fisher Scientific) was employed for profiling and identification of metabolites formed in HLM. LC separation was carried out using a mobile phase comprised of 0.1% formic acid (v/v) in water (solvent A) and 0.1% formic acid in acetonitrile (v/v) (solvent B). A linear gradient of solvent A starting at 95% to 10% from 0 to 23 min followed by remaining at 10% for 3 min before returning to 95%. The total run time was 30 min and flow rate was 0.3 mL/min. The mass spectrometer was operating in the positive electrospray ionization mode in the m/z range of 100-1000. Capillary temperature was at 275°C. Capillary voltage was at 46V. UV profile of racemic amlodipine and its

DMD #55400

metabolites in HLM incubations was acquired at 245 nm for semi-quantitative estimation of relative abundance of metabolites to the parent drug. Their full scan MS and MSⁿ data were acquired using a data-dependent method for metabolite structure characterization. The same LC/MS instrument and method except for a short LC run time (13 min) were employed for determination of relative amounts of the dehydrogenation metabolite (M9) in the time-course, HLM inhibition and metabolism in CYP experiments. In the analysis, full scan MS data was acquired and then extracted ion chromatogram at m/z 409 was generated. Peak area corresponding to M9 was calculated as the measurement of the relative abundance of M9.

Results and Discussions

Identification of Amlodipine Metabolites Formed in HLM. LC/MS analysis showed that a total of nine metabolites were formed in HLM incubations with 30 μ M racemic amlodipine or S-amlodipine (Table 1). M9 and M10 exhibited relatively higher abundances and accounted for 5.9% and 3.2% of racemic amlodipine, respectively, based on an UV profile (Fig. 1A). Other metabolites were detectable only by LC/MS (Supplementary Fig. S1). Protonated molecular ions and MSⁿ spectra of the parent drug and its metabolites are summarized in Table 1. Based on mass spectral interpretation and comparisons with those reported in the literature (Suchanova et al., 2006 and 2008), metabolite structures and their formation pathways are proposed in Fig. 1C. For example, the structure of M9 was ascertained based on the comparison of its MS/MS spectrum (Fig. 1B) to that of the parent drug (Supplementary Fig 1) as well as that of the amlodipine pyridine metabolite reported previously. Amlodipine dehydrogenation to M9 was the major metabolic pathway in HLM. M9 underwent further metabolism including oxidative deamination to M10, *O*-demethylation to M1 and *O*-dealkylation to M4. In addition, amlodipine underwent *O*-demethylation to M6 and monohydroxylation to M3, M5 and M8 (Table 1 and Fig.

DMD #55400

1C), which constituted minor pathways in HLM since the metabolites were not displayed in the UV profile (Fig. 1A). Metabolic profiles of racemic amlodipine and *S*-amlodipine in HLM were similar except that *O*-demethylation leading to M1 and M6 was not observed for *S*-amlodipine (Table 1). The major metabolic pathway observed in HLM is consistent with the major clearance pathway of amlodipine in human subjects: amlodipine dehydrogenation followed by oxidations to multiple metabolites (Beresford et al., 1988a; Stopher et al., 1988).

Time Course of Amlodipine Metabolism in HLM. To optimize incubation conditions for assessing the contribution of CYP enzymes to amlodipine dehydrogenation, racemic amlodipine and *S*-amlodipine were incubated at a lower concentration (1 μ M) with HLM, respectively. Metabolite profiles were determined and time-courses of the M9 formation were semi-quantified by LC/MS. Under the condition investigated, the formation of M9 in HLM increased linearly with increasing incubation time within 15 min. No sequential metabolites of M9 were detected, reinforcing the idea that M9 is the intermediate to other pyridine derivatives during amlodipine metabolism. Disappearance of either racemic amlodipine or *S*-amlodipine was less than 76% of the initial concentrations following 15 min incubations. Based on these data, 1 μ M substrate concentration and 13 min incubation time were chosen for the subsequent CYP reaction phenotyping experiments. It was expected that the formation of M9 under the condition is in a linear range.

Identification of CYP Enzyme Responsible for Amlodipine Dehydrogenation. As shown in Fig. 2, the formation of M9 from amlodipine or *S*-amlodipine was NADPH-dependent and nearly completely inhibited by ketoconazole, a potent inhibitor of both CYP3A4 and CYP3A5, and CYP3cide, a potent and selective inhibitor of CYP3A4 (Walsky et al., 2012). Chemical inhibitors of other major CYP enzymes, including sulfaphenazole (CYP2C9),

DMD #55400

benzylirvanol (CYP2C19), quinidine (CYP2D6), montelukast (CYP2C8), furafylline (CYP1A2) and Thio-TEPA (CYP2B6), had no or minimal inhibitory effect on amlodipine dehydrogenation. Similarly, results from metabolism of racemic amlodipine and *S*-amlodipine by a panel of expressed CYP enzymes showed that CYP3A4 was the single CYP enzyme catalyzing the formation of M9 (Fig. 3).

To further confirm that CYP3A5 has no or minimal catalyzing activity toward amlodipine dehydrogenation, the relative formation rate of M9 from racemic amlodipine in CYP3A4 and CYP3A5 was compared to that of 1'-OH-midazolam from midazolam in CYP3A4 and CYP3A5. Midazolam is a substrate of both CYP3A4 and CYP3A5. Results from the current study showed that the formation rates of 1'-OH-midazolam in expressed CYP3A4 and CYP3A5 were 3.96 and 7.21 (nmol/min/nmol CYP), respectively, the relative formation of 1'-OH-midazolam in CYP3A4 and CYP3A5 was 100:182, which are in agreement with those reported in the literature (Christensen et al., 2011; Li et al., 2012). In contrast, the relative formation of M9 in CYP3A4 and CYP3A5 was 100:11. When CYP3sdie, a CYP3A4 specific inhibitor, was co-incubated with CYP3A4 and CYP3A5, the M9 formation in CYP3A4 was greatly reduced to the levels in CYP3A5, while CYP3cide had no effect on the M9 formation in CYP3A5. These results indicate that CYP3A4 is responsible primarily for the formation of M9 via amlodipine dehydrogenation. CYP3A5 and other CYP enzymes have no or little role in catalyzing amlodipine dehydrogenation. The differences of amlodipine exposures observed between CYP3A5 non-expressers and expressers (Kim et al., 2006; Zuo et al., 2013) could be due to differences of CYP3A4 expressions between the two groups since CYP3A5 has minimal, if at all, effect on the *in vitro* metabolism of amlodipine (Fig. 2 and 3). The *in vitro* data also support an early clinical observation that blood pressure response to amlodipine among high-risk African-

DMD #55400

Americans appears to be determined by CYP3A4, but not CYP3A5 genotypes (Bhatnagar et al., 2010).

In summary, racemic amlodipine and *S*-amlodipine were slowly metabolized in HLM. Amlodipine dehydrogenation to the pyridine metabolite (M9) was the single most important metabolic pathway in HLM; M9 further underwent oxidative deamination, *O*-demethylation and *O*-dealkylation. These in vitro metabolism data are consistent with amlodipine metabolism and disposition observed in vivo in human. The data derived from amlodipine metabolism in expressed CYP and HLM with CYP inhibitors indicate that CYP3A4, not CYP3A5, is the primary contributor to amlodipine dehydrogenation. Metabolite profiles and CYP reaction phenotyping data of a racemic mixture and *S*-isomer of amlodipine were very similar, consistent with pharmacokinetics of racemic amlodipine and *S*-amlodipine in human. These findings suggest that the observed clinical drug-drug interactions between amlodipine and CYP3A4/5 inhibitors are mediated by CYP3A4 rather than CYP3A5. In addition, polymorphic expressions of CYP3A5 would not affect the pharmacokinetic variability of amlodipine and the blood pressure response to amlodipine in human.

DMD #55400

Authorship Contributions:

Participated in research design: M. Zhu and Chen

Conducted experiments: Y. Zhu, Li and Wang

Contributed new reagents or analytic tools: Du

Performed data analysis: Y. Zhu, Li, M. Zhu, Chen

Wrote or contributed to the writing of the manuscript: Y. Zhu, Tang, Weiqing Chen and M. Zhu

DMD #55400

References:

Abernethy DR (1991) Amlodipine: pharmacokinetic profile of a low-clearance calcium antagonist. *J Cardiovasc Pharmacol* **17** Suppl 1:S4-7.

Beresford AP, McGibney D, Humphrey MJ, Macrae PV, Stopher DA (1988a) Metabolism and kinetics of amlodipine in man. *Xenobiotica* **18**:245-254.

Beresford AP, Macrae PV, Stopher DA (1988b) Metabolism of amlodipine in the rat and the dog: a species difference. *Xenobiotica* **18**:169-182.

Bhatnagar V, Garcia EP, O'Connor DT, Brophy VH, Alcaraz J, Richard E, Bakris GL, Middleton JP, Norris KC, Wright J, Hiremath L, Contreras G, Appel LJ, Lipkowitz MS (2010) CYP3A4 and CYP3A5 polymorphisms and blood pressure response to amlodipine among African-American men and women with early hypertensive renal disease. *Am J Nephrol.* **31**:95-103.

Christensen H, Hestad AL, Molden E, Mathiesen L (2011) CYP3A5-mediated metabolism of midazolam in recombinant systems is highly sensitive to NADPH-cytochrome P450 reductase activity. *Xenobiotica* **41**:1-5.

Faulkner JK, McGibney D, Chasseaud LF, Perry JL, Taylor IW (1986) The pharmacokinetics of amlodipine in healthy volunteers after single intravenous and oral doses and after 14 repeated oral doses given once daily. *Br J Clin Pharmacol.* 1986 Jul;22(1):21-25

Glesby MJ, Aberg JA, Kendall MA, Fichtenbaum CJ, Hafner R, Hall S, Grosskopf N, Zolopa AR, Gerber JG (2005) Pharmacokinetic interactions between indinavir plus ritonavir and calcium channel blockers. *Clin Pharmacol Ther* **78**:143-153.

Guengerich FP, Brian WR, Iwasaki M, Sari MA, Bäärnhielm C, Berntsson P (1991) Oxidation of dihydropyridine calcium channel blockers and analogues by human liver cytochrome P-450 IIIA4. *J Med Chem* **34**:1838-1844.

DMD #55400

Kim KA, Park PW, Lee OJ, Choi SH, Min BH, Shin KH, Chun BG, Shin JG, Park JY (2006) Effect of CYP3A5*3 genotype on the pharmacokinetics and pharmacodynamics of amlodipine in healthy Korean subjects. *Clin Pharmacol Ther* **80**:646-656.

Kim BH, Kim JR, Kim MG, Kim KP, Lee BY, Jang IJ, Shin SG, Yu KS (2010) Pharmacodynamic (hemodynamic) and pharmacokinetic comparisons of S-amlodipine gentsiate and racemate amlodipine besylate in healthy Korean male volunteers: two double-blind, randomized, two-period, two-treatment, two-sequence, double-dummy, single-dose crossover studies. *Clin Ther* **32**:193-205.

Lee JE, van Heeswijk R, Alves K, Smith F, Garg V (2011) Effect of the hepatitis C virus protease inhibitor telaprevir on the pharmacokinetics of amlodipine and atorvastatin *Antimicrob Agents Chemother* **55**:4569-4574.

Li X, Song X, Kamenecka TM, Cameron MD (2012) Discovery of a highly selective CYP3A4 inhibitor suitable for reaction phenotyping studies and differentiation of CYP3A4 and CYP3A5. *Drug Metab Dispos* **40**: 803-809

Stopher DA, Beresford AP, Macrae PV, Humphrey MJ (1988) The metabolism and pharmacokinetics of amlodipine in humans and animals *J Cardiovasc Pharmacol*. **12 Suppl 7**:S55-59.

Suchanova B, Sispera L, Wsol V (2006) Liquid chromatography-tandem mass spectrometry in chiral study of amlodipine biotransformation in rat hepatocytes *Anal Chim Acta*. **573-574**:273-283.

Suchanova B, Kostianinen R, Ketola RA (2008) Characterization of the in vitro metabolic profile of amlodipine in rat using liquid chromatography-mass spectrometry *Eur J Pharm Sci* **33**:91-99.

Walsky RL, Obach RS, Hyland R, Kang P, Zhou S, West M, Geoghegan KF, Helal CJ, Walker GS, Goosen TC, Zientek MA (2012) Selective mechanism-based inactivation of CYP3A4 by CYP3cide (PF-04981517) and its utility as an in vitro tool for delineating the relative roles of CYP3A4 versus CYP3A5 in the metabolism of drugs. *Drug Metab Dispos* **40**:1686-1697.

Zhang YP, Zuo XC, Huang ZJ, Cai JJ, Wen J, Duan DD, Yuan H (2013) CYP3A5 polymorphism, amlodipine and hypertension. *J Hum Hypertens* [Epub ahead of print]

DMD #55400

Zuo XC, Zhou YN, Zhang BK, Yang GP, Cheng ZN, Yuan H, Ouyang DS, Liu SK, Barrett JS, Li PJ, Liu Z, Tan HY, Guo R, Zhou LY, Xie YL, Li ZJ, Li J, Wang CJ, Wang JL (2013) Effect of CYP3A5*3 polymorphism on pharmacokinetic drug interaction between tacrolimus and amlodipine. *Drug Metab Pharmacokinet* [Epub ahead of print]

DMD #55400

Legends for figures

Fig. 1. Amlodipine metabolite profile in HLM. (A) UV profile of metabolites of racemic amlodipine in HLM (30 μ M, 60 min, 2 mg protein/mL). (B) MS² spectrum and the structures of the pyridipine metabolite (M9). (C) Proposed structures and formation pathways of amlodipine metabolites in HLM.

Fig. 2. Inhibition of the formation of M9 from racemic amlodipine and S-amlodipine in HLM by CYP inhibitors

Fig. 3. Relative abundance of M9 formed in incubations of racemic amlodipine and S-amlodipine with recombinant human CYP enzymes.

DMD #55400

Table 1. Summary of amlodipine metabolites detected in HLM by LC/MS

Metabolite	RT (min)	Identity	MH ⁺	MS ⁿ Spectral Data	racemic amlodipine	S-amlodipine
M1	10.06	P-2H-CH ₂	393	MS ² : 376, 350, 332, 314, 304; MS ³ (332): 304, 286	√	–
M3	11.79	P + O	425	MS ² : 379, 336, 294, 364; MS ³ (336): 318, 304, 180	√	√
M4	12.02	P-2H-C ₂ H ₄ NH-C ₂ H ₄	336	MS ² : 318,286 ; MS ³ (318): 286	√	√
M5	12.06	P + O	425	MS ² : 417, 390, 379, 336, 294 ; MS ³ (336): 318,304,286,181	√	√
M6	12.06	P-CH ₂	395	MS ² :352, 334, 306,180; MS ³ (180): 163,144	√	–
M8	12.71	P + O	425	MS ² : 390, 379, 336, 294, 364; MS ³ (336): 318, 304, 248,181	√	√
M9	13.57	P-2H	407	MS ² : 390, 364, 346, 318, 286; MS ³ (346): 318, 286.	√	√
M10	17.88	P-2H-NH+O	408	MS ² : 346,318, 286, 390; MS ³ (346): 318, 286	√	√
M12	18.38	P-2H-NH+2O-2H	422	MS ² : 376, 346, 318, 286; MS ³ (346): 318, 286	√	√
P	15.02	Amlodipine	409	MS ² : 392, 346, 348, 320, 294, 238; MS ³ (392): 360, 346	√	√

Fig. 1

DMD Fast Forward. Published on December 3, 2013 as DOI: 10.1124/dmd.113.055400
This article has not been copyedited and formatted. The final version may differ from this version.

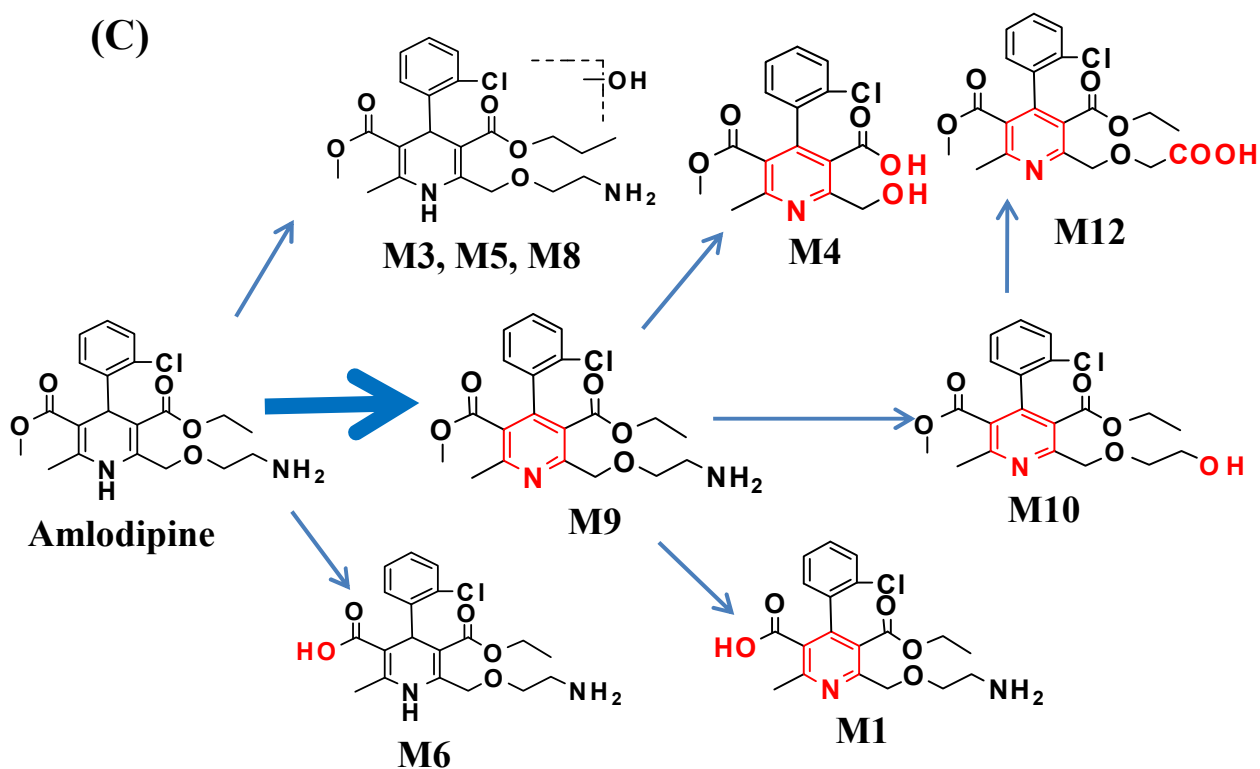
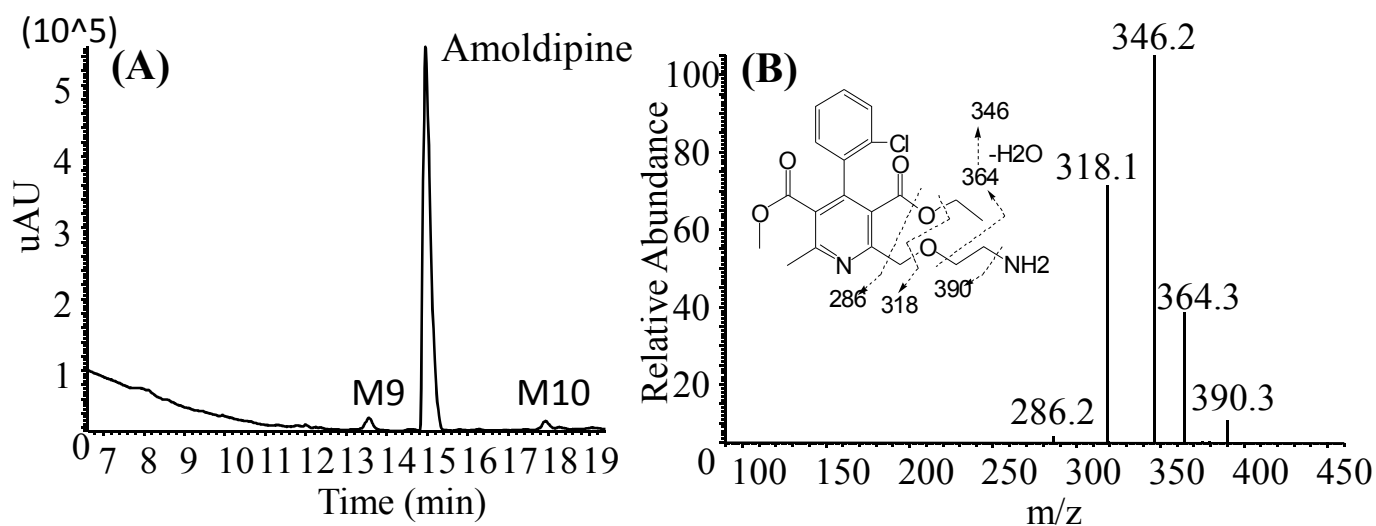


Fig. 2.

DMD Fast Forward. Published on December 3, 2013 as DOI: 10.1124/dmd.113.055400
This article has not been copyedited and formatted. The final version may differ from this version.

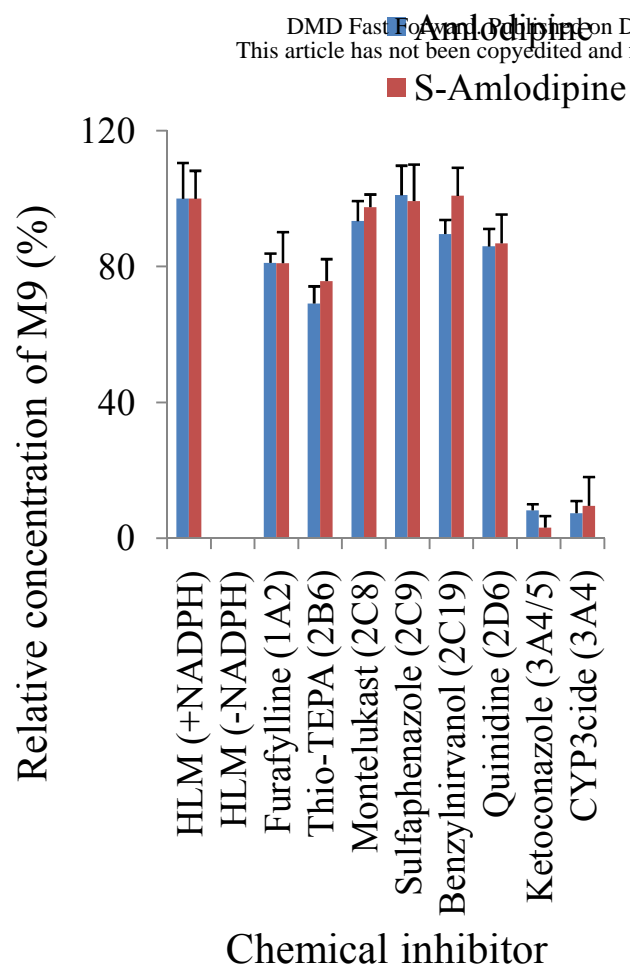


Fig. 3.

DMD Fast Forward. Published on December 3, 2013 as DOI: 10.1124/dmd.113.055400
This article has not been copyedited and formatted. The final version may differ from this version.

